

Shear Transformation Zone Activation During Deformation in Bulk Metallic Glasses Characterized Using a New Indentation Creep Technique

J. B. Puthoff¹, H. B. Cao¹, J.E. Jakes^{1,2}, P. M. Voyles^{1,3}, and D. S. Stone^{1,3}

¹Materials Science Program, University of Wisconsin – Madison, Madison WI 53706,
U.S.A.

²USDA Forest Product Laboratory, Madison WI 53726, U.S.A.

³Materials Science & Engineering, University of Wisconsin – Madison, Madison WI
53706, U.S.A.

ABSTRACT

We have developed a novel type of nanoindentation creep experiment, called broadband nanoindentation creep (BNC), and used it to characterize the thermal activation of shear transformation zones (STZs) in three BMGs in the Zr-Cu-Al system. Using BNC, material hardness can be determined across a wide range of strain rates (10^{-4} to 10 s⁻¹) in a single experiment at room temperature. This data can be used to characterize the kinetics of deformation, including the free energy function (ΔG) for thermally-activated deformation. We have found that the activation energy agrees with the theory of Johnson and Samwer, in which $\Delta G \propto [(\tau_c - \tau)/\tau_c]^{3/2}$, where τ is the flow stress and τ_c is the flow stress at 0K. In the context of their model, we estimate that the volume of an STZ is ~ 100 -300 atomic volumes and the activation energies for low-stress deformation are 5-10 eV. From these measurements, it is possible to reproduce the temperature dependence of the flow stress.

BACKGROUND

Plastic deformation in metallic glasses (MGs) is thought to be the result of cooperative rearrangements of atoms in susceptible regions of the glass under the influence of an applied shear stress [1-4]. This reorganization could be restricted to a single atom making a diffusive jump [1], or it could encompass a few dozen atoms changing to a sheared configuration [2-4]. Rearrangements of the second type are the basis for the shear transformation zone (STZ) [5] description of MG defects. The unique deformation properties that MG alloys exhibit [6] are the consequence of the dynamics of STZ activation and, in turn, the structural details of the glass.

With the discovery of bulk metallic glasses (BMGs) [7], there is a need for mechanical characterization techniques that provide insight into deformation mechanisms present in MGs. Nanoindentation is a common technique [8] which is typically used to determine the “rate-independent” hardness (H_0) and the elastic modulus (E) of samples of material whose geometry or properties preclude conventional testing, such as embedded phases or brittle materials. Less well-known are the uses of nanoindentation to study the time-dependent (creep) properties of materials, which can provide insight into the nature and dynamics of plastic deformation. These techniques can be broadly classified under the heading “nanoindentation creep” [9, 10], and have recently been applied to MGs [11-13].

The dynamics of defect-based MG deformation imply a constitutive plastic deformation law in which the overall strain rate ($\dot{\epsilon}$) is proportional to the rate of defect activation, such as

$$\dot{\epsilon} = \dot{\epsilon}_0(c) \exp\left[-\frac{\Delta G(\tau)}{k_B T}\right], \quad (1)$$

where $\dot{\epsilon}_0$ is a material-dependent constant (with units s^{-1}), k_B is Boltzmann's constant, and T is the temperature. In general, $\dot{\epsilon}_0$ depends on the concentration (c) of defects in the alloy, but will be constant if isostructural deformation is assumed. ΔG is the energy barrier to STZ activation, which depends on the shear stress (τ). The exact shape of ΔG is not known, but a form like

$$\Delta G(\tau) = \Delta G_0 \left(\frac{\tau_c - \tau}{\tau_c} \right)^n \quad (2)$$

captures the overall behavior of a number of models of MG deformation. ΔG_0 is the energy barrier at low stresses, τ_c is the flow stress at 0K, and n is a power-law exponent. Proposed values for n include: 1 [1], 3/2 [4], or 2 [2]. A complete phenomenological description of MG deformation can be produced by determining the parameters $\dot{\epsilon}_0$, ΔG_0 , τ_c , and n . The ultimate meaning of these parameters is determined by the physics of the particular model.

Here we present the results of a nanoindentation creep study of three BMGs in the Zr-Cu-Al system: $Zr_{54}Cu_{38}Al_8$, $Zr_{45}Cu_{49}Al_6$, and $Zr_{36}Cu_{58}Al_6$ using a novel indentation creep technique we call broadband nanoindentation creep (BNC). BNC captures the instantaneous material hardness (which is a measure of the instantaneous yield stress) over a range of strain rates spanning 5 decades. The BNC data can be used to determine the set of phenomenological deformation parameters of Equations 1 and 2. These parameters, considered in the context of a specific MG deformation model [4], provide insight into the physical process underlying MG defect activation.

EXPERIMENTAL

The three BMG specimens were suction-cast [14] in a water-cooled copper mold from a melt of pure (99.99 at.% or greater) components under a high-purity Ar atmosphere. From the bottom of each 3 mm diameter ingot (where the cooling rate is highest), we cut a cylindrical piece 3 mm in length for resonant ultrasound spectroscopy (RUS) [15] and nanoindentation experiments. Another adjacent piece of each ingot was used for XRD, DSC, and TEM analysis in order to verify the glassy nature of the ingot [16]. We mechanically polished one face of each nanoindentation specimen to a mirror (0.05 μm) finish, both to remove any surface oxides and to produce a flat, perpendicular surface for indentation.

We conducted all nanoindentation experiments on a Hysitron (Minneapolis, MN, USA) Triboindenter with a Berkovitch indenter and a Quesant (Agoura Hills, CA, USA) atomic force microscope (AFM) attachment. The electronics package of this instrument provides the data-collection rates required for BNC measurements, with the caveats noted below. RUS experiments were conducted on an apparatus incorporating two Olympus (Waltham, MA, USA) Panametrics shear-wave transducers, a function generator, and an oscilloscope.

The BMG specimens were each tested in eight BNC experiments. In each test, the indenter tip/specimen was loaded to 10 mN in 0.05 s, held for a prescribed period: $t_{creep} = 0.01, 0.05, 0.1, 0.5, 2, 10, \text{ or } 50$ s, and unloaded. The unloading times (t_{unload}) varied between tests; they were as brief as 0.01 s (for $t_{creep} = 0.01$ s) or 0.05 s (for $t_{creep} = 0.1$ and 0.5 s) and as long as 0.5–1 s (for $t_{creep} = 2, 10, 50$ s). We performed two experiments with $t_{creep} = 0.05$ s, one with $t_{unload} = 0.05$ s and the other with $t_{unload} = 0.01$ s, in order to assess the effects of electronic filtering on the test data. In the tests for which t_{creep} was 0.5 s or greater, the unloading segment

of the experiment was halted at 2 mN and allowed to dwell at this load for an interval between 6 and 50 s in order to calculate drift in the instrument. We imaged the residual indents with the AFM attachment and used ImageJ image analysis software (<http://rsb.info.nih.gov/ij/>) to determine the residual indent areas (A_0) [17].

Two corrections to the displacement signal ($h(t)$) from the Triboindenter are needed. First, a second-order, low-pass filter is used to reduce noise on the displacement signal, and the frequency response of this filter must be compensated for. Second, a correction for thermal drift for long experiments ($t_{creep} \geq 2$ s) is necessary. From the corrected nanoindentation data, instantaneous hardness ($H(t)$) and indentation strain rate ($\dot{\epsilon}_H(t)$) data for BNC may be extracted from the peak-load hold segment of an experiment. H is given by the instantaneous load ($P(t)$) divided by the instantaneous projected indent area ($A(t)$). A cannot be measured directly, but can be modeled accurately using the A_0 values from the 8 individual nanoindentation creep experiments, a simple model of indenter penetration [10], and relations determined from finite element simulations of the indentation of von Mises solids [18, 19].

It is typically assumed that, during creep, \sqrt{A} increases in proportion to h [20, 21]. This assumption is incorrect, because the proportionality factor between \sqrt{A} and depth changes as a result of the drop in hardness that takes place during creep [19]. In our analysis, we choose to work with the purely plastic component of depth (h_p), and take $\sqrt{A} \propto h_p$ raised to some other exponent (ζ_p), which differs from 1 but approaches 1 for soft materials ($H_0 \ll E$). We inferred ζ_p for each MG using the A_0 values from indents with different total creep times.

From $A(t)$, an indentation strain rate can be defined as $\dot{\epsilon}_H(t) \equiv d \ln \sqrt{A(t)} / dt$, giving $H(\dot{\epsilon}_H)$. The properties of $H(\dot{\epsilon}_H)$ reflect the constitutive behavior of the MG in the fashion of Equation 1. In order to interpret our results in this context, we must (i) convert hardness to flow stress (σ), then to shear flow stress, and (ii) convert the strain rate sensitivity of the hardness ($m_H \equiv \partial \ln H / \partial \ln \dot{\epsilon}_H |_{h,T}$) to that of the shear flow stress ($m_\tau \equiv \partial \ln \tau / \partial \ln \dot{\epsilon} |_{\epsilon,T}$). We use $H \approx 3\sigma$, following the results in [8, 22], $\sigma = 2\tau$, and $m_H \approx 0.95m_\tau$ [18].

RESULTS AND DISCUSSION

The $H(\dot{\epsilon}_H)$ data from the BNC experiments conducted on all three alloys with $t_{creep} = 50$ s are shown in Figure 1. A single experiment provides information on material properties spanning 5+ decades in strain rate. The values of hardness for the alloys drop by 10-15% over the 50 s duration of the creep portion of the experiment. At locations indicated by the arrows, H drops systematically and the curves become concave down. This departure might be related to pop-in behavior observed during loading. Pop-in has been attributed to the nucleation and operation of shear bands and is expected to be prevalent at low strain rates [23-25].

In order to generate the phenomenological deformation parameters from $H(\dot{\epsilon}_H)$, we need to extract the form of the activation energy. We do this using the activation volume, $V^* \equiv -\partial \Delta G / \partial \tau |_{\epsilon,T}$, or

$$V^*(\tau) = k_B T \left. \frac{\partial \ln \dot{\epsilon}}{\partial \tau} \right|_{\epsilon,T} = \frac{k_B T}{m_\tau \tau}. \quad (3)$$

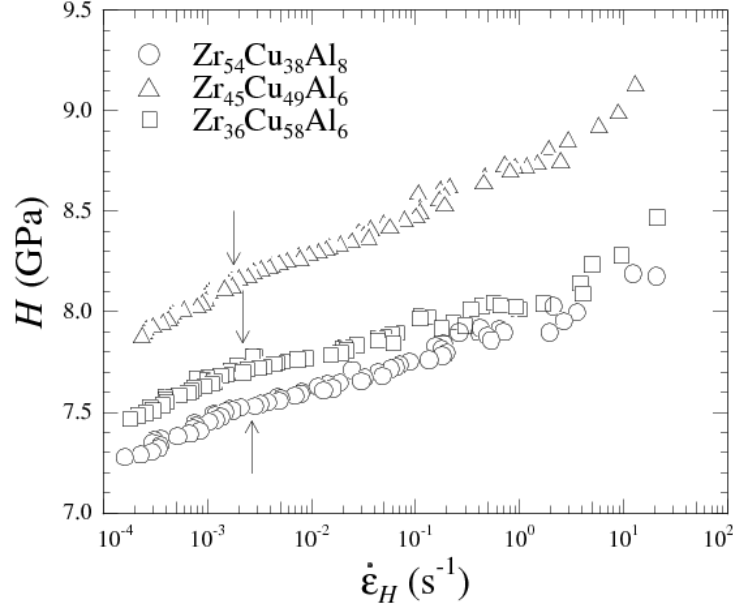


Figure 1. $H(\dot{\epsilon}_H)$ curves for the three BMGs derived from the BNC experiments with $t_{creep} = 50$ s.

Following Equation 2, we take V^* to be a power law with exponent $n - 1$. V^* is $3\Delta G_0/2\tau_c$ at low stresses. Figure 2 is a plot of $[V^*(\tau)]^2$ for all three alloys, in which we have normalized V^* to the average atomic volume in the MG (Ω) and the shear flow stress to the (room-temperature) shear modulus ($\mu_{0, R.T.}$) from RUS. The linearity of these curves is an indication that $3/2$ is an acceptable value for n , though we find that n may be as large as 2 and still display good linear correlation. From the data in Figure 2, other phenomenological parameters may be extracted, such as τ_c and ΔG_0 . These properties are summarized in Table I. The rate parameter $\dot{\epsilon}_0$ was determined from a fit (incorporating the other parameters) of the derived $\tau(\dot{\epsilon})$ data to Equation 1.

Table I. phenomenological deformation parameters determined from BNC

Alloy	$\tau_c / \mu_{0, R.T.}$	n	ΔG_0 (eV)	$\dot{\epsilon}_0$ (s^{-1})
Zr ₅₄ Cu ₃₈ Al ₈	0.041 ± 0.001	1.75 ± 0.25	7.2 ± 0.6	1.4×10^7
Zr ₄₅ Cu ₄₉ Al ₆	0.041 ± 0.001	1.75 ± 0.25	5.0 ± 0.4	3×10^6
Zr ₃₆ Cu ₅₈ Al ₆	0.035 ± 0.001	1.75 ± 0.25	10.7 ± 0.8	2×10^5

As a physical model, we adopt the Johnson-Samwer theory of STZ operation in MGs [4]. In this theory, the irreversible transformation of an STZ is equivalent to the transition between minima on the potential energy surface of the glass. Johnson and Samwer propose a specific form for the barrier separating minima,

$$\Delta G(\tau) = 4R\mu_0(T)\gamma_c^2 \left(\frac{\tau_c - \tau}{\tau_c} \right)^{3/2} \lambda \Omega_{STZ}, \quad (4)$$

where R ($\approx 1/4$) is the “fold ratio”, λ (≈ 3) is a correction factor for matrix effects, and Ω_{STZ} is the volume of the flow defect. γ_c is the strain in the individual defects, estimated to be $\pi\tau_c/2\mu_0(T)$. Using Equation 4, we calculate the product $\gamma_c\Omega_{STZ}$ in the range 0.11-0.28 nm³, or 6-19 atomic volumes. Heggen *et al.* [26] have estimated $\gamma_c\Omega_{STZ}$ as 8-10 atomic volumes from compression creep of a Pd-based BMG at low stress and high temperatures, and Yang, Wadsworth, and Nieh [27] measure $\gamma_c\Omega_{STZ} = 0.19$ nm³ using nanoindentation near T_g in an Au-based BMG. We have determined Ω_{STZ} to be equivalent to $(160\pm 10)\Omega$ for Zr₅₄Cu₃₈Al₈, $(100\pm 10)\Omega$ Zr₄₅Cu₄₉Al₆, and $(300\pm 20)\Omega$ for Zr₃₆Cu₅₈Al₆. These values are in good agreement with measurements made over a smaller range of strain rate on similar alloys using the same model [28].

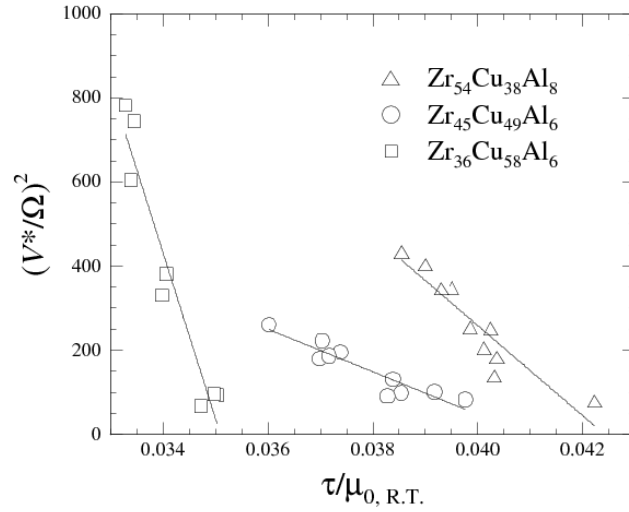


Figure 2. $[V^*(\tau)]^2$ curves for the three BMGs, extracted from the data in Figure 1.

These parameters reproduce the shape of the temperature-dependence of the flow stress implied by Equation 1. Figure 3 shows these derived $\tau(T)$ curves superimposed on similar data determined from about 30 BMGs and collected by Johnson and Samwer [4]. To generate these curves, the temperature-dependence of μ_0 has been inferred from the data published in [15]. The positive offset between our calculation and the data could be eliminated by changing the proportionality constant between H and σ , but that disagrees with other data.

CONCLUSION

The activation of shear transformation zone (STZ) defects in 3 bulk metallic glasses has been characterized using broadband nanoindentation creep, a novel technique which can measure material properties over a wide range of strain rates (10^{-4} to 10 s⁻¹). With these results, all of the deformation parameters in a simple, phenomenological, deformation model may be determined. We find that the power law exponent for the activation energy is in the range 1.5-2, and that the activation energies at low stresses are 5-10 eV. These parameters reproduce the shape of the temperature dependence of the flow stress. Within the Johnson-Sawmer STZ model, the volume of the flow defects is 100-300 atomic volumes.

This work was supported by the U.S. National Science Foundation (CMMI-0824719).

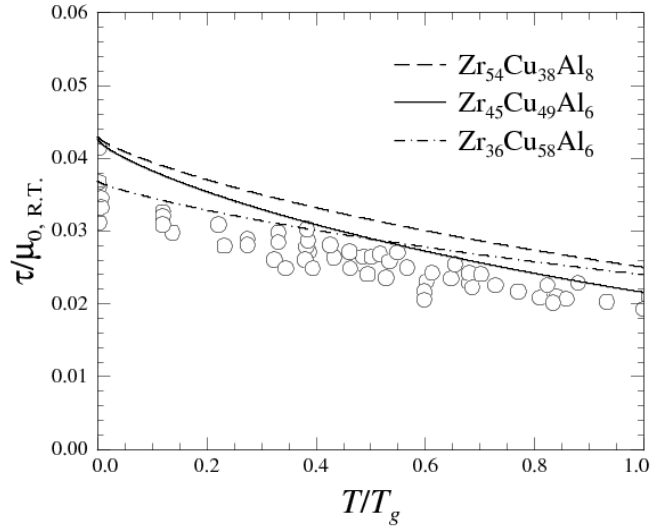


Figure 3. $\tau(T)$ curves, constructed from the parameters in Table I. The transition temperature (T_g) for $\text{Zr}_{54}\text{Cu}_{38}\text{Al}_8$, $\text{Zr}_{45}\text{Cu}_{49}\text{Al}_6$, and $\text{Zr}_{36}\text{Cu}_{58}\text{Al}_6$ is 677K, 706K, and 750K, respectively.

REFERENCES

- [1] F. Spaepen, *Acta Metall.* **25**, 407 (1977).
- [2] A. S. Argon, *Acta Metall.* **27**, 47 (1979).
- [3] J. S. Langer, *Phys. Rev. E* **70**, 041502 (2004).
- [4] W. L. Johnson, and K. Samwer, *Phys. Rev. Lett.* **95**, 195501 (2005).
- [5] M. L. Falk, and J. S. Langer, *Phys. Rev. E* **57**, 7192 (1998).
- [6] C. A. Schuh, T. C. Hufnagel, and U. Ramamurty, *Acta Mater.* **55**, 4067 (2007).
- [7] W. L. Johnson, *MRS Bulletin* **24**, 42 (1999).
- [8] C. A. Schuh, and T. G. Nieh, *J. Mater. Res.* **19**, 46 (2004).
- [9] W. B. Li, and R. Warren, *Acta Metall. Mater.* **10**, 3065 (1993).
- [10] D. S. Stone, and K. B. Yoder, *J. Mater. Res.* **9**, 2524 (1994).
- [11] J. B. Puthoff *et al.*, *Mater. Res. Soc. Symp. Proc.* vol. 1048E, 1048 (2007).
- [12] D. Fátay, J. Gubicza, and J. Lendvai, *J. Alloy Comp.* **434-435**, 75 (2007).
- [13] W. H. Li *et al.*, *Mater. Sci. Eng. A* **478**, 371 (2008).
- [14] H. Cao *et al.*, *Acta Mater.* **54**, 2975 (2006).
- [15] Z. Zhang *et al.*, *J. Mater. Res.* **22**, 364 (2007).
- [16] J. Hwang and P. M. Voyles, unpublished (2007).
- [17] J. E. Jakes *et al.*, *J. Mater. Res.* **23**, 1113 (2008).
- [18] A. A. Elmustafa, S. Kose, and D. S. Stone, *J. Mater. Res* **22**, 926 (2007).
- [19] D. S. Stone, and A. A. Elmustafa, *Mater. Res. Soc. Symp. Proc.* Vol. 1049, 1049 (2008).
- [20] D. Jang, and M. Atzmon, *J. Appl. Phys.* **93**, 9282 (2003).
- [21] F. Wang, P. Huang, and K. W. Xu, *Appl. Phys. Lett.* **90**, 161921 (2007).
- [22] K. E. Prasad, R. Raghavan, and U. Ramamurty, *Scripta Mater.* **57**, 121 (2007).
- [23] C. A. Schuh, and T. G. Nieh, *Acta Mater.* **51**, 87 (2003).
- [24] W. H. Li *et al.*, *J. Mater. Res.* **21**, 75 (2006).
- [25] F. Yang *et al.*, *Acta Mater.* **55**, 321 (2007).
- [26] M. Heggen, F. Spaepen, and M. Feuerbacher, *Mater. Sci. Eng. A* **375-377**, 1186 (2004).
- [27] B. Yang, J. Wadsworth, and T.-G. Nieh, *Appl. Phys. Lett.* **90**, 061911 (2007).
- [28] D. Pan *et al.*, *PNAS* **105**, 14769 (2008).